Acta Physiol Plant (2016) 38:259
DOI 10.1007/s11738-016-2276-6

ORIGINAL ARTICLE

Self-preserving lognormal volume-size distributions of starch granules in developing sweetpotatoes and modulation of their scale parameters by a starch synthase II (SSII)

Ming Gao[1] · Qun Xia[2] · Akwe W. Akwe[2] · Lakeisha Stewart[2] · Glory M. Ashu[2] · Victor Njiti[2]

Received: 29 March 2016 / Revised: 22 June 2016 / Accepted: 3 October 2016 / Published online: 12 October 2016

Abstract

Main conclusion **Starch granule size distributions in plant tissues, when determined in high resolution and specifiedproperly as a frequency function, could provide useful information on the granule formation and growth.**

Abstract To better understand genetic control of physical properties of starch granules, we attempted a new approach to analyze developmental and genotypic effects on morphology and size distributions of starch granules in sweetpotato storage roots. Starch granules in sweetpotatoes exhibited low sphericity, many shapes that appeared to be independent of genotypes or developmental stages, and non-randomly distributed sizes. Granule size distributions of sweetpotato starches were determined in high resolution as differential volume-percentage distributions of volume-equivalent spherical diameters, rigorously curve-fitted to be lognormal, and specified using their geometric means $\bar{x}^*$ and multiplicative standard deviations s^* in a $\bar{x}^* \times /(\text{multiply/divide})s^*$ form. The scale ($\bar{x}^*$) and shape ($\bar{s}^*$) of these distributions were independently variable, ranging from 14.02 to 19.36 μm and 1.403 to 1.567, respectively, among 22 cultivars/clones. The shape (s^*) of granule lognormal volume-size distributions of sweetpotato starch were found to be highly significantly and inversely correlated with their apparent amylose contents. More importantly, granule lognormal volume-size distributions of starches in developing sweetpotatoes displayed the same self-preserving kinetics, i.e., preserving the shape but shifting upward the scale, as those of particles undergoing agglomeration, which strongly indicated involvement of agglomeration in the formation and growth of starch granules. Furthermore, QTL analysis of a segregating null allele at one of three homoeologous starch synthase II loci in a reciprocal-cross population, which was identified through profiling starch granule-bound proteins in sweetpotatoes of diverse genotypes, showed that the locus is a QTL modulating the scale of granule volume-size distributions of starch in sweetpotatoes.

Keywords Starch granules · Granule size distributions · Multiplicative specification · Self-preserving size distributions · Starch granule-bound proteins · Soluble starch synthase II

Abbreviations

AIC	Akaike information criterion
CV	Coefficient of variation
DAT	Days after transplanting
ESZ	Electrical sensing zone
K–S	The Kolmogorov–Smirnov test
MALDI-TOF/TOF	Matrix-assisted laser desorption/ionization time-of-flight
MV	Mie or modified Mie-calculated geometric means
QTL	Quantitative trait locus
SGP	Starch granule-bound protein
SSII	Starch synthase II

Communicated by L. A. Kleczkowski.

Electronic supplementary material The online version of this article (doi:10.1007/s11738-016-2276-6) contains supplementary material, which is available to authorized users.

✉ Ming Gao
migao@pvamu.edu

[1] Cooperative Agricultural Research Center, Prairie View A&M University, MS 2008, P.O. Box 519, Prairie View, TX 77446, USA

[2] Center for Biotechnology and Genomics, Alcorn State University, 1000 ASU Drive, Lorman, MS 39096, USA

Introduction

Chemically, starch refers to two types of homoglucan polymers: (1) the linear or sparsely branched amylose and (2) the highly branched amylopectin. Physically, starch in plant photosynthesis and storage tissues exists as granules that assume many shapes (Shannon and Garwood 1984; Singh et al. 2003), including spheres, ellipsoids, polyhedrons, platelets, cubes, cuboids, and irregular tubules. Thus, starch synthesis involves at least two phases, the enzymatic synthesis of amylose and amylopectin, and the formation and growth of starch granules from amylose, amylopectin, and minor components of lipid and proteins. Most of the physicochemical, biochemical, and structural properties of amylose, amylopectin, and starch granules have been extensively studied (reviewed in BeMiller and Whistler 2009; Buléon et al. 1998; Copeland et al. 2009; Hoover 2001; Lindeboom et al. 2004; Perez and Bertoft 2010; Tester and Debon 2000; Tester et al. 2004; Zobel 1988). Moreover, in recent decades, molecular genetic and genomics studies have substantially advanced our understanding of amylose and amylopectin biosynthesis, and genetic regulations of these processes (reviewed in Baldwin 2001; Ball and Morell 2003; Emes et al. 2003; Hannah and James 2008; James et al. 2003; Jeon et al. 2010; Keeling and Myers 2010; Smith 2001; Smith et al. 2005; Tetlow 2011; Tomlinson and Denyer 2003; Zeeman et al. 2010). However, very little is known about the genetic control of physical properties, especially the size of starch granules in plants.

Starch granules in plant tissues exist in a range of sizes that vary in number frequencies and volume (or mass) percentages, i.e., displaying a certain size distribution. Although size distributions of starch granules in plant storage tissues have been well recognized and described (reviewed in Lindeboom et al. 2004), they have been rarely defined using distribution specifications. Instead, granule sizes of starch from many plant storage tissues were often described using a simple average of or range of 'diameters' (reviewed in Buléon et al. 1998; Hoover 2001; Lindeboom et al. 2004; Moorthy 2002; Shannon and Garwood 1984). In some cases, this parameter has been simplified as the arithmetic mean of the microscopically measured largest dimensions of two-dimensional (2D) granule images (Goering et al. 1973; Li et al. 2011), for which the number of observed granules was even as low as 15 (Wang et al. 1993). Regardless of the population size of sampled granules, such a simple average of 'diameters' or the largest dimensions apparently cannot accurately define the distributed sizes of heterogeneously shaped starch granules, often with very low sphericity, in a plant tissue. To address the issue of low granule sphericity, some researchers have used transformed spherical equivalent diameters for calculation of the average diameter (Lindeboom et al. 2004); however, the problem of biased average weighting due to different granule number frequencies for various size categories remains. Others have simply specified ranges of the granule size distributions (Chen et al. 2003; Dai 2009) or used the distribution mean volume or mean equivalent spherical diameter (weighted by number, volume, or surface area) assuming a normal distribution (Edwards et al. 2008; Karlsson et al. 1983; Li et al. 2008; Park et al. 2009; Wilson et al. 2006). These varying specifications of starch granule sizes make it very difficult to meaningfully compare reported granule sizes of starches from different or the same sources in various studies, which may have hindered our efforts to understand genetic control of starch granule size distributions in plant tissues.

In this study, we attempted a new approach to analyze developmental and genotypic effects on morphology and size distributions of starch granules in sweetpotato storage roots for a better understanding of the genetic control of physical properties of starch granules. To properly define granule size distributions, we determined granule sizes of starch in sweetpotato storage roots as differential volume-percentage distributions of volume-equivalent spherical diameters in high resolution, and specified the fitted lognormal distributions using a universally comparable multiplicative two-parameter specification. We analyzed granule volume-size distributions of starch from more than 65 cultivars/clones that have diverse genetic background, and kinetics of starch granule size distributions in developing sweetpotatoes. We demonstrated for the first time that granule lognormal volume-size distributions in developing sweetpotatoes shared the signature self-preserving kinetics of size distributions of particles undergoing agglomeration. In addition, a single-locus QTL analysis using a reciprocal-cross population segregating for a null allele at one of three homoeologous starch synthase II (SSII, both granule-bound and soluble) loci showed that the *SSII* locus is a QTL modulating the scale of granule lognormal volume-size distributions of starch in sweetpotatoes, demonstrating a direct genotypic effect of starch synthesis enzymes on granule size distributions.

Materials and methods

Plant materials

The initial seeding sweetpotatoes or vine cuttings of cultivars/clones used in this study were kindly provided by the sweetpotato breeding and genetics program of North Carolina State University (Covington, Hernandez, Diane, O'

Henry, Hannah, NC-Japanese, and Murasaki-29), the US-Vegetable Lab, SC (Excel, SC1149-19, the Excel/SC1149-19 reciprocal-cross population, and W364), and the USDA-ARS Plant Genetic Resources Conservation Unit, Griffin, GA (all remaining cultivars/clones). Storage roots used for starch extractions were sampled from freshly harvested uncured storage roots from plants that were grown in neighboring rows in the field or individually in pots for three seasons.

Starch isolation and analyses of apparent amylose contents

For starch preparation, about ~20 g of sweetpotato slices (1–2 mm thick) were randomly sampled out of 1 kg of slices from freshly harvested whole sweetpotatoes of desired size grades (<US No. 1 petite, US No. 1 petite, the US No. 1 and >US No. 1 sizes), chopped and finely ground in 20–25 mL of cold water using a Warring Chopper/Grinder. Starch in the slurry was then filtered through two layers of Miracloth (pore size: 22–25 μm) into a 250-mL beaker and allowed to settle for approximately 30 min. The settled starch was recovered, resuspended in approximately 30 mL of cold water, and transferred to a centrifuge tube. Starch was pelleted by centrifugation for 5 min at 6000×*g* speed. Colored gel-like materials overlaying the packed white starch granules were scraped using a spatula. This raw starch preparation was then washed twice in a cold buffer [62.5 mM Tris-HCl (pH 6.8), 10 mM EDTA, and 0.14 M SDS], three times in cold water, and once in cold acetone (approximately 15 mL) by repeated resuspension and centrifugation. The purified starch was air dried, aliquoted, and stored in a sealed tube at −20 °C. Three 20–25 mg samples from each of the starch preparations were used for analyses of the apparent amylose content with a Megazyme Amylose/Amylopectin Assay Kit (Megazyme, Wicklow, Ireland).

SDS-PAGE analysis of SGPs and peptide identification

To extract granule-bound proteins, a 50-mg starch sample was suspended in 200 μL of an extraction buffer [62.5 mM Tris-HCl (pH 6.8), 0.35 M SDS, and 0.39 M DTT] and boiled for 15 min in a screw-cap microcentrifuge tube. The boiled mixtures were cooled to room temperature and centrifuged for 15 min at 16,000×*g*. About 60 μL of the supernatant (~85 to 105 μg total protein) was transferred to a new microfuge tube, reduced with 15 mM tributylphosphine for 1 h at room temperature, alkylated with 17 mM iodoacetamide for 1.5 h at room temperature, and finally combined with 15 μL of 5× or 60 μL of 2× loading buffer for SDS-PAGE analysis. For confirmation of the SGP4 null phenotype, supernatants of about 60 μL each from two or three individual extractions of 50-mg samples from the same starch preparation were combined, and precipitated using the ProteoPrep® Protein Precipitation Kit (Sigma-Aldrich, St. Louis, MO, USA). The protein pellets were reconstituted in 60 μL of the extraction buffer, reduced and alkylated as above. Treated SGPs of about 85–105 μg from regular extractions, and of about 180–270 μg from combined 2X or 3X extractions for confirmation of SGP4 null phenotype were fractionated using a 50 g L^{-1} (5 %) acrylamide (30:0.135 acrylamide:bisacrylamide) stacking gel [50 mM Tris-HCl (pH 6.8) and 3.47 mM SDS] and a 150 g L^{-1} (15 %) acrylamide (30:0.135 acrylamide:bisacrylamide) separating gel [0.375 mM Tris-HCl (pH 7.8) and 3.47 mM SDS] of large format (16 cm × 2 0 cm × 1.5 mm gel) as previously reported, with modifications (Zhao and Sharp 1996). After separation, proteins were visualized with silver staining using a SilverQuest kit (Invitrogen, Carlsbad, CA, USA). Protein identification of individual peptide bands cut out of gels by the matrix-assisted laser desorption/ionization time-of-flight (MALDI-TOF)/TOF) peptide map fingerprint was carried out using the Pick'n Post service of Alphalyse (Palo Alto, CA, USA).

Analysis of starch granule sizes

A Multisizer™ 3 Coulter Counter was used for reported granule volume-size analyses of various sweetpotato starches. The instrument was fitted with a 100-μm aperture tube and calibrated to have a k_d of 125 when using 200 mL of 50 g L^{-1} Lithium chloride in Methanol as an electrolyte. The control mode was set to detect the sizes of 250,000–300,000 particles with automatic current and gain settings. The pulse to size conversion was set at 300 size bins ranging from 2.3 to 300 μm, with log-diameter bin spacing. For each starch preparation, two 5.0-g samples were individually suspended in 5 mL Methanol in a 50-mL conical centrifuge tube and fully dispersed using several pulses of low intensity ultrasound (12–24 W cm^{-2}) from a handheld ultrasonic processor (UPH50 with a MS2 sonotrode; Hielscher Ultrasound Technology, NJ, USA). Using a 1.5-mL transfer pipette, several drops (0.2–0.5 mL) of the starch suspension were applied to 200 mL of 50 g L^{-1} LiCl-Methanol electrolyte under constant stirring in a 250-mL sample cup to reach a concentration corresponding to a ~5 to 6 % reading of the index meter. The sizing process was monitored manually and paused to flush the aperture tube if clogging occurred. After completion of each sizing measurement, the sample cup was emptied, washed, and refilled with 200 mL of fresh electrolyte solution for the next measurement. Each 5-mL starch suspension was drop sampled twice for sizing differential

volumes of more than 500,000 starch granules, and more than 1 million starch granules from two independent suspension samples of each starch preparation were thus sized. This scheme of double drop-sampling each from two suspension samples for one starch preparation was adopted after this sampling scheme was found to yield sizing results showing no significant difference from those from one sizing measurement each of four independent suspensions of 5-g samples from a starch preparation.

The differential volume-size distributions from the four independent volume-sizing analyses of a starch preparation were averaged to yield a differential volume-size distribution in log scale using the instrument software. All of these averaged volume-size distributions were curve-fitted to be lognormal, and thus specified using their instrument-calculated geometric mean ($\bar{x}^*$) of volume-equivalent spherical diameters in μm and geometric standard deviation (s^*) in the $\bar{x}^* \times /$(multiply or divide)s^* specification form following the recommendation of Limpert et al. (2001). The two specification parameters $\bar{x}^*$ and s^* are mathematically 'back-transformed' values of the classic graphic mean μ and the graphic standard deviation σ of lognormal distributions, i.e., $\bar{x}^* = e^{\mu}$ and $s^* = e^{\sigma}$.

The laboratory analysis service Microtrac Inc. (York, PA, USA) was contracted for the laser diffraction size analyses of starch granules using an S3500 laser diffraction particle size analyzer. Starch granules were suspended in water and analyzed in triplicate in the volume-size range from 0.0215 to 1408 μm equivalent spherical diameters for a 30-s run time. For imaging size analyses, at least 10 digital images covering more than 1000 granules for each cultivar were taken from several granule suspensions prepared from 2 to 3 starch samples isolated from different storage roots of the same cultivar. The maximal dimensions of imaged granules were determined with ImageJ (Version 1.41) image processing software. The number of starch granules in each size group was counted. The number percentage of starch granules of a particular size group was plotted against the granule diameter to obtain the distributions of sizes of starch granules from a particular cultivar.

Microscopy imaging

Bright-field microscopy images of sweetpotato starch granules were taken from starch granules suspended in 12 M ethanol using an Olympus DP71 digital camera on a BX51 microscope. Polarized-light microscopy images of sweetpotato starch granules were taken from starch granules suspended in water using an Olympus DP 70 digital camera on a Leitz Diaplan microscope under polarized light.

Statistical analyses

The Prism 5 statistics and graphing software package (GraphPad Software, La Jolla, CA, USA) was used for all statistical analyses other than those performed by the Multisizer 3 software package. The EastFit 5.5 Professional package (Mathwave Technologies, http://www.mathwave.com) was used for all distribution curve fitting.

Results

Starch granules from genotypically diverse sweetpotato cultivars/clones exhibited similar types of shapes and surface morphologies, but diverse size distributions

To understand genotypic effects on granule morphology and size distributions of sweetpotato starches, we first assessed the diversity of the physical properties of starches in storage roots of 50 genotypically diverse sweetpotato cultivars/clones. Figure 1 shows representative microscopy images and differential volume-size distributions of starch granules in sweetpotato storage roots of some of the surveyed cultivars/clones. Starch granules in sweetpotato storage roots from the same or different cultivar/clone varied broadly in shape, surface morphology, and sizes. More predominant granule shapes, as observed in Fig. 1a, include spheres, hemispheres, ellipsoids, cubes, cuboids, platelets, polyhedrons, and many irregular types. The granule sphericity of starches from all the surveyed cultivars/clones was generally very low. In addition, surface cavities and wrinkles of various sizes and shapes were observed, particularly on many of the larger granules. However, no significant differences in types of granule shapes or surface morphology were observed among starches from various cultivars/clones or from different developmental stages of the same cultivar/clone, although there was sometimes a discernible difference in the frequencies of certain shapes or surface morphology types (Fig. S1). Thus, the shape and surface morphology of starch granules in sweetpotato storage roots appeared to be independent of genotypes or developmental stages.

A new approach was attempted to accurately determine and properly specify size distributions of starch granules having very low sphericity in sweetpotato storage roots. Granule volume sizes of various sweetpotato starches were measured in high resolution by quadruple sampling of more than 250,000 particles each using the Coulter method. The differential volume-size distributions from the quadruple measurements for each starch preparation were averaged (standard deviations of the averages ranging from

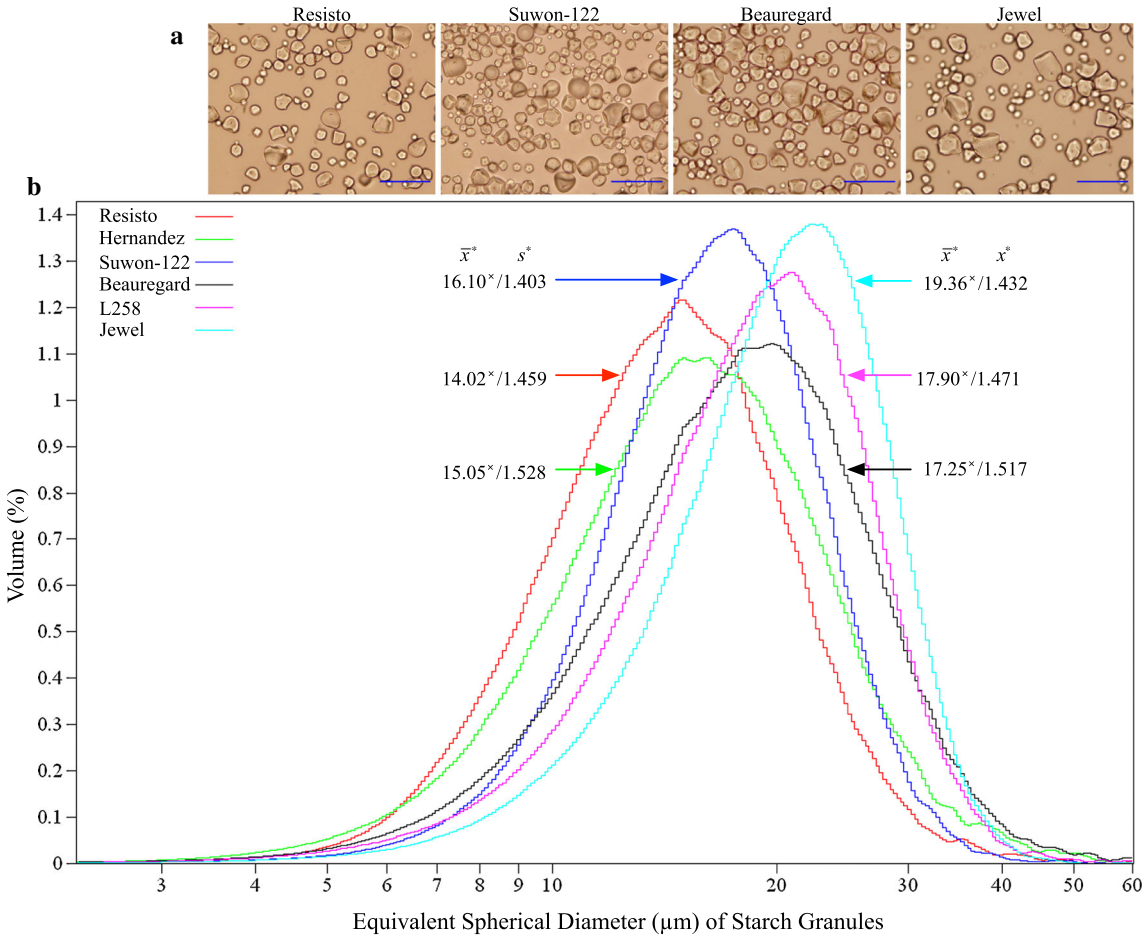

Fig. 1 Representative granule morphology and lognormal differential volume-size distributions of starch from sweetpotato storage roots. **a** Microscopic images of representative starch granules from storage roots of four cultivars. The *scale bars* represent 100 μm. Higher-resolution images of starch granules from four cultivars, and of representative shapes of starch granule were provided in the supplemental Fig. S1. **b** Granule lognormal differential volume-size distributions of starches from storage roots of six selected cultivars/clones. Samples of starches prepared from storage roots grown in neighboring rows were dispersed in 50 g L^{-1} LiCl-Methanol solution and sized for differential volumes in 300 size bins from 2.3 to 300 μm of equivalent spherical diameter using the Coulter method. Each distribution curve was derived from an average of four independent sizing measurements of more than 250,000 particles each and smoothed by grouping seven adjacent size bins. These lognormal distributions were specified by their respective scale estimator $\bar{x}^*$ (the geometric mean of volume-equivalent spherical diameters in μm) ×/(multiply/divide) their shape factor s^* (geometric standard deviation)

0.0019 of Excel to 0.017 of Murasaki-29), and were then curve-fitted and evaluated for goodness of fit to the lognormal and normal distributions using the Kolmogorov–Smirnov (K–S) test. The probabilities (P, K–S test) of all these distributions following a three-parameter (scale, shape, and location factors, i.e., μ, σ, and γ, respectively) lognormal distribution ranged from 0.98 to 1, and the maximum difference (D, K–S test) in the cumulative fraction of these distributions from theoretical distributions was less than 0.02, indicating an almost perfect fit. However, the location parameters (γ) of these fitted lognormal distributions, which defined starting points for the support set of the distribution, were all negative, ranging from −47.76 to −1.12. These virtual size thresholds at the left of the fitted curves were likely fitting artifacts that could compensate for the asymmetrical presence of tails, i.e., the very small percentage volumes of very large granules, at the right side of the curves, and thus may not have any physiological relevance. All the averaged differential volume-size distributions also fit the two-parameter lognormal distributions very well ($P = 0.25$–0.99; $D < 0.05$), while only some of them fit normal distributions equally well. The preference for the lognormal over the normal distribution for all datasets was further confirmed by the Akaike information criterion (AIC). All of the granule differential volume-size distributions of sweetpotato starch were thus approximated as two-parameter (μ, σ) lognormal distributions, and were specified using their geometric means ($\bar{x}^*$) and geometric standard deviations (s^*) in a multiplicative $\bar{x}^* \times /s^*$ form, following the recommendation of Limpert et al. (2001). The specifications of these averaged granule lognormal volume-size distributions of sweetpotato starch,

Table 1 Properties of granule lognormal differential volume-size distributions of starches from some sweetpotato cultivars/clones and apparent amylose contents of these starches

Cultivar/clones	Multiplicative specification of volume-size distributions $\bar{x}^*$ ×/ s^*	Amylose content (% of starch)
Excel	14.19 ×/ 1.454	22.11 ± 0.13
Resisto	14.02 ×/ 1.459	20.05 ± 0.30
Centennial	14.28 ×/ 1.518	19.48 ± 0.21
Hannah	14.08 ×/ 1.567	18.11 ± 0.32
Hernandez	15.05 ×/ 1.528	20.01 ± 0.42
Covington	15.21 ×/ 1.469	21.22 ± 0.47
Murasaki-29	15.66 ×/ 1.474	20.64 ± 0.53
Diane	15.61 ×/ 1.509	19.86 ± 0.41
Hidry	15.68 ×/ 1.497	21.57 ± 0.26
Suwon-122	16.10 ×/ 1.403	29.52 ± 0.52
Picadito	16.07 ×/ 1.513	20.32 ± 0.37
Tis-70683	16.36 ×/ 1.491	18.44 ± 0.25
W369	16.70 ×/ 1.482	20.21 ± 0.13
Koto-puki	17.43 ×/ 1.427	20.70 ± 0.13
Beauregard	17.25 ×/ 1.517	19.80 ± 0.33
O'Henry	17.73 ×/ 1.485	19.56 ± 0.14
Hayman	17.87 ×/ 1.515	19.73 ± 0.27
L258	17.90 ×/ 1.471	20.05 ± 0.55
SC1149-19	17.69 ×/ 1.471	20.96 ± 0.55
GA90-16	18.34 ×/ 1.484	20.54 ± 0.68
Jewel	19.36 ×/ 1.432	18.34 ± 0.30
NC-Japanese	19.36 ×/ 1.480	20.77 ± 0.08

Starches were isolated from sweetpotatoes of US No. 1 size grade, which were grown in neighboring rows in the same season. The distribution specification for each cultivar/clone was from the distribution averaged from those of four independent sizing measurements of each starch preparation

along with their apparent amylose contents, from selected cultivars/clones are summarized in Table 1.

The scale estimators ($\bar{x}^*$) of these lognormal distributions had a relatively broad range from 14.02 to 19.36 μm in equivalent spherical diameters, whereas their shape factors (s^*) varied within a narrow range from 1.403 to 1.567. Figure 1b illustrates three pairs of granule lognormal volume-size distributions of sweetpotato starches from six cultivars/clones, representing the ranges of $\bar{x}^*$ and s^* of all the observed distributions. Each pair shared a similar s^* (1.403/1.432, 1.459/1.471, and 1.528/1.517) with statistically insignificant differences but varied substantially in $\bar{x}^*$ (16.10/19.36, 14.02/17.90, and 15.05/17.25, respectively). On the other hand, granule lognormal volume-size distributions of starches from some other sweetpotato cultivars/clones (e.g., Excel vs. Centennial and Resisto vs. Hanna; Table 1) shared similar $\bar{x}^*$, but differed significantly in s^*. The shape (s^*) and scale ($\bar{x}^*$) of granule lognormal volume-size distributions of sweetpotato starch were thus independently variable and may have different physiological and genetic implications. Furthermore, the shape (s^*) but not scale ($\bar{x}^*$) of granule volume-size distributions of sweetpotato starch was highly significantly and inversely correlated with their apparent amylose contents (Pearson $r^2 = 0.3402$, $P = 0.0045$), but not with the total starch content or any starch thermal properties (Table S2). In other words, the amylose content of sweetpotato starch granules appeared to significantly affect the spread of the granule size distribution.

The microscopy imaging and laser diffraction particle sizing methods were also attempted for comparison. Despite many trials, the variance of repeated sizing of the same starch preparation using both methods was too large to allow for any meaningful or accurate analyses. The ratio of the standard deviation to the arithmetic mean of the means of the maximal surface lengths of starch granules, i.e., coefficient of variation (CV), for three or four repeated image size analyses of a starch preparation could be as large as 30 % (data not shown). Additionally, the CV, or the ratio of the standard deviation to the arithmetic mean of Mie or modified Mie-calculated geometric means (MV) of equivalent spherical diameters for granule volume-size distributions, for four or five repeated laser diffraction sizing analyses of two starch preparations from Excel and

Table 2 Properties of lognormal differential-volume-size distributions of starch granules from some sweetpotato cultivars/clones, measured with the angular light scattering diffraction method

Cultivar/clones	Instrument output specification parameters MV ± SD (σ_g)	Estimated multiplicative specification parameters $\bar{x}^*$ ×/ s^*
Excel		
1	11.39 ± 4.40	10.62 ×/ 1.28
2	13.84 ± 3.87	13.33 ×/ 1.20
3	14.50 ± 5.27	13.63 ×/ 1.28
4	17.88 ± 6.05	16.94 ×/ 1.24
5	19.19 ± 5.89	18.35 ×/ 1.22
SC1149-19		
1	16.27 ± 6.00	15.27 ×/ 1.27
2	20.09 ± 7.26	18.89 ×/ 1.26
3	14.62 ± 5.66	13.63 ×/ 1.28
4	19.62 ± 5.91	19.10 ×/ 1.21
Beauregard	16.47 ± 5.99	15.48 ×/ 1.26
Suwon-122	16.74 ± 4.94	16.06 ×/ 1.21
Convington	16.98 ± 4.90	16.31 ×/ 1.20
Jewel	23.41 ± 7.11	22.40 ×/ 1.22
Diane	15.84 ± 6.10	14.78 ×/ 1.28
Picadito	12.97 ± 4.96	12.11 ×/ 1.28
SC103	17.79 ± 6.31	16.77 ×/ 1.25
SC85	19.31 ± 7.29	18.07 ×/ 1.27
SC77	13.93 ± 4.73	13.19 ×/ 1.24
SC65	12.07 ± 4.74	11.23 ×/ 1.28
XL93	13.43 ± 4.66	12.69 ×/ 1.25
XL79	19.25 ± 6.73	18.17 ×/ 1.25
XL47	20.31 ± 5.36	19.64 ×/ 1.19
XL7	13.55 ± 5.12	12.68 ×/ 1.27

Starch samples were all isolated from sweetpotatoes of US No. 1 size grade, which were grown side-by-side. The Instrument-output specification parameters for Excel and SC1149-19 were the arithmetic average of three measurements each of the five or four independent samples of the same starch preparations from Excel or SC1149, respectively. Those for all other cultivar/clones were the arithmetic average of three measurements of one sample from the respective starch preparation. The multiplicative specification parameters were estimated using the following formula (Limpert et al. 2001): $\bar{x}^* = \mathrm{MV}/\sqrt{\omega}$, $s^* = \exp(\sqrt{\log(\omega)})$, where $\omega = 1 + (\sigma_g/MV)^2$

MV Mie or modified Mie-calculated mean diameter in microns of the "volume distribution", which represents the center of gravity of the distribution, *SD* (σ_g) standard deviation, also known as the graphic standard deviation (σ_g), which is one measure of the width of the distribution, but not an indication of variability for multiple measurements

SC1149-19 could still reach 15–20 % ($\overline{\mathrm{MV}} \pm \mathrm{SD}$ 15.36 ± 3.16 and 17.65 ± 2.64 μm for repeated sizing of the Excel and SC1149-19 starch, respectively; Table 2). Moreover, both the imaging and laser diffraction sizing methods lacked sufficient resolution to distinguish differences in shapes of granule differential volume-size distributions of starch. The shape (s^*) of granule lognormal volume-size distributions of starches from 16 sweetpotato cultivars/clones, which were calculated using data from laser diffraction sizing analyses (Table 2), showed no statistically significant differences, contrary to the sizing results obtained using the high-resolution Coulter method (below).

Granule lognormal volume-size distributions of starches at different developmental stages of sweetpotato storage roots preserved the shape, but shifted the scale

To understand the kinetics of starch granule growth in developing sweetpotato storage roots, we examined granule volume-size distributions of starch from storage roots of a breeding line SC1149-19 at varying developmental ages or grown under different conditions. As shown in Fig. 2, the granule lognormal volume-size distributions of starches from storage roots at three bulking stages, spanning 70 days of early formation, middle bulking, and late

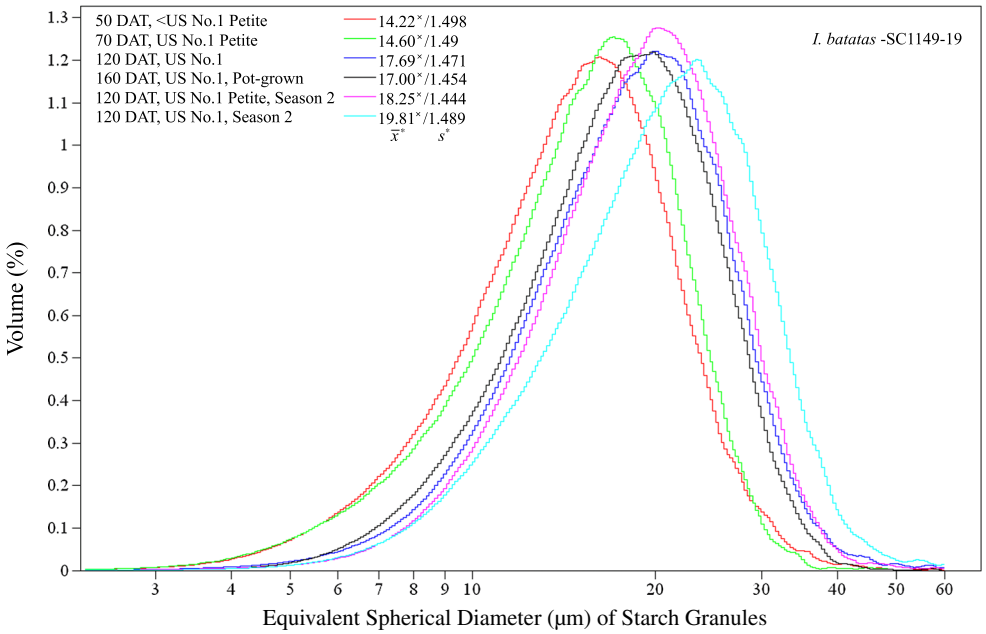

Fig. 2 Self-preserving granule lognormal volume-size distribution of starch in developing sweetpotato storage roots. The granule lognormal volume-size distributions of starch in storage roots of a breeding line SC1149-19 at three or two bulking stages in two growing seasons and in those grown in pots remained invariant in shape, displaying s^* values having no statistically significant differences, but shifted upward in scale ($\bar{x}^*$) as the bulking of storage roots progressed. This kinetics approximated the characteristic self-preserving state in particle agglomeration. Starch was purified from field-grown storage roots at two or three of the following bulking stages during two growing season: <US No. 1 petite size (3.8–5.7 cm in diameter and 7.6–17.8 cm in length) at 50 DAT, US No. 1 petite at 70 DAT, and US No. 1 size (<8.9 cm in diameter, 7.6–22.8 cm in length, and <567 g in weight), and from pot-grown ones of US No. 1 size at 160 DAT. The sizing of starch granules, averaging and smoothing of these distribution curves were carried out as described before

harvest stages, and from those grown in pots or in a second season at comparable harvest stages displayed statistically insignificant differences (~1.5 % CV) in their shape (s^*). However, the scale ($\bar{x}^*$) of the granule volume-size distributions expanded as the bulking of storage roots progressed, from 14.22/14.60 μm in storage roots of small sizes (≤3.81–5.7 cm in diameter and ≤7.6–17.8 cm in length, US No. 1 petite sizes) at 50–70 days after transplanting (DAT) to 17.69 μm in those of commercial sizes (US No. 1, <8.9 cm in diameter, 7.6–22.8 cm in length, and <567 g in weight) at 120 DAT of the harvest stage during one growing season, and from 18.25 μm in storage roots of US No. 1 petite sizes to 19.81 μm in those of US No. 1 sizes at 120 DAT in a second season. Additionally, the granule volume-size distributions of starches from storage roots grown under different growth conditions at comparable harvest stages also varied in the scale ($\bar{x}^*$) (i.e., 17.00,17.69 and 19.81 μm for those grown in pots, and in fields during two seasons, respectively), while preserving the shape (s^*). The same kinetics (i.e., of shifting the scale while preserving the shape) were also observed among the granule lognormal volume-size distributions of starches from storage roots of the cultivar Excel at two developmental ages each in two growth seasons, and those of another cultivar Picadito at two developmental stages over two seasons (Supplemental Fig. S2). For this study, the Excel and SC1149-19 clones were always grown side-by-side, and harvested at the same time.

Please note that the size of a sweetpotato storage root alone does not necessarily represent its developmental ages. Both the growth time after transplanting and the sizes were thus used to roughly define the physiological and developmental ages of sweetpotato storage roots. However, at the same DAT, smaller-sized storage roots were reasonably assumed to be at a younger developmental stage.

An SSII homoeolog was genetically associated with modulating the scale ($\bar{x}^*$) of the granule lognormal volume-size distributions of starches in sweetpotato storage roots.

A microscopic survey of sweetpotato starches revealed that starch from two parents, Excel and SC1149-19, of a reciprocal-cross population exhibited visually discernible differences in granule size distributions. The Excel starch contained on average lesser-sized granules than that the SC1149-19 starch, as could be readily observed by comparing polarized-light microscopy images (Fig. 3a) representative of starch granule populations from the two lines. Additionally, similar to potato starch granules, sweetpotato starch granules extinguished polarized light of a certain direction and were thus anisotropic. For accurate quantitative comparison, starch samples from storage roots of the

two parents and their reciprocal-cross progenies, which were grown in neighboring rows and harvested at the same time, were carefully sized using the Coulter method. As shown in Fig. 3a, the granule lognormal volume-size distributions of starches from Excel and SC1149-19 differed significantly in their scale $\bar{x}^*$ (14.75 vs. 18.25 μm, respectively), which was consistent with our microscopic observations. However, the two distributions shared essentially the same shape, having s^* values (1.455 vs. 1.444, respectively) that did not differ significantly. These two starch samples from the two lines also did not exhibit any significant difference in their amylose content (18.9 vs. 19.5 %). Moreover, the starch samples from storage roots of the two lines grown side-by-side in another season displayed no statistically significant differences in their apparent amylose contents (Table 1), gelatinization and retrogradation thermal properties (Supplemental Table S2), amylose/amylopectin ratio (0.28 vs. 0.27, Supplemental Table S2)', and amylopectin side chain profiles (data not shown). Thus, the only identifiable difference between starches from storage roots of Excel and SC1149-19 was the scale of their granule lognormal volume-size distributions.

To understand genetic variations underlying the phenotypic differences in the $\bar{x}^*$ of granule lognormal volume-size distributions of starches from the two lines, we first compared profiles of SGPs in storage roots of these two lines using a modified SDS-PAGE procedure. As shown in Fig. 3b, about 10–12 major bands could be resolved from extracts of SGPs from the two lines. Twelve slices of these resolved bands from SC1149-19 or Excel were excised for peptide sequencing. Table 3 and S1 summarize successful identification of nine major polypeptides and their probable orthologs in other species. Three major features of the two SGP profiles were notable. First, the SGPs were predominated by a disproportionately heavy band of 60 kDa (SGP9), and multiple neighboring bands above and below the major band, which became a heavy smear in the region spanning from approximately 50 to 68 kDa when silver staining was developed sufficiently to allow light bands of higher molecular weights (particularly SGP1) to be observed. Four major bands from the region, i.e., SGP8, -9, -10, and -12, were all identified as granule-bound SSIs (GBSSIs) by peptide sequencing. These multiple (>6) polypeptide bands of 50–68 kDa were thus most likely all GBSSI paralogs or homoeologs. Additionally, the neighboring band SGP7 of about 70 kDa was identified as an ortholog of a potato starch synthase (a maize GBSSI ortholog), but only by seven Mr-matched peptides, and low protein score and sequence coverage of 12 % (Table 3). The starch synthase type of SGP7 may need further clarification, particularly because the apparent size and migration position of SGP7 on SDS-PAGE were more similar to those of maize or rice SSI than to those of GBSSI. The large number of resolved GBSSI bands (>6) and the disproportionate amount of at least one GBSSI band (SGP9) were consistent with our previous estimate of three GBSSI paralogs per diploid constituent genome in the hexaploid sweetpotato, i.e., nine copies in total (Gao et al. 2010). The varying intensities of these resolved GBSSI bands indicated that these GBSSI homoeologs and paralogs were unevenly expressed in sweetpotato storage roots.

The second feature of the two SGP profiles was the presence of only one type of starch branching enzymes (SBE), the SBEIIs, i.e., SGP1 (~110 kDa) and SGP5 (~97 kDa). Note that the SGP1 band, although very faint on the particular gel, was confirmed to be present in SC1149-19 by repeated SDS-PAGE analyses of multiple independent starch samples. The faint band at ~76 kDa (SGP6) between SGP5 and SGP7 in the SGP file of SC1149-19 was most likely a degraded polypeptide because repeated peptide sequencing of the band failed, and the band was not present in all starch samples from SC1149-19 storage roots. Attempts at peptide sequencing of a small-sized band (SGP11 of ~15 kDa, not shown) and a very faint band (the SGP3 slice) at the bottom of SGP2 also failed. The third feature, which was possibly the most important feature of the two SGP profiles, was the absence of the SGP4 band (~99 kDa) from starch granules of Excel. This null SGP4 phenotype in Excel was repeatedly confirmed by SDS-PAGE analyses of multiple starch samples purified from storage roots of both parental lines grown under different conditions over three seasons, and by overloading of 2 and 3 times of protein extracts from starches of Excel for all these analyses. SGP4 from SC1149-19 and SGP2 (~107 kDa) was identified as SSII orthologs of maize and wheat SSIIa. The SGP2 and SGP4, and the SGP1 and SGP5, were most likely two separate groups of homoeologs, SSIIa and SBEII, respectively. The two homoeologs of each group were resolvable by SDS-PAGE as they were encoded by homoeologous loci in different constituent diploid genomes of the hexaploid sweetpotato genome, and differed slightly in amino acid sequence and in length so as to have differential electric mobility. This differential electric mobility of homoeolgs should be similar to what was well demonstrated in the hexaploid wheat (Rahman et al. 1995). Moreover, the much stronger intensity of the SGP2 band indicated that it may not be homogeneous and could contain two SSIIa homoeologs having an undetectable size difference and very limited sequence variations.

To investigate the possible genetic associations of the loss of one of at least three homoeologous SSII enzymes with the downsizing of the scale of the granule lognormal volume-size distribution of starch in Excel, we genotyped 43 progenies from the reciprocal-cross population at the

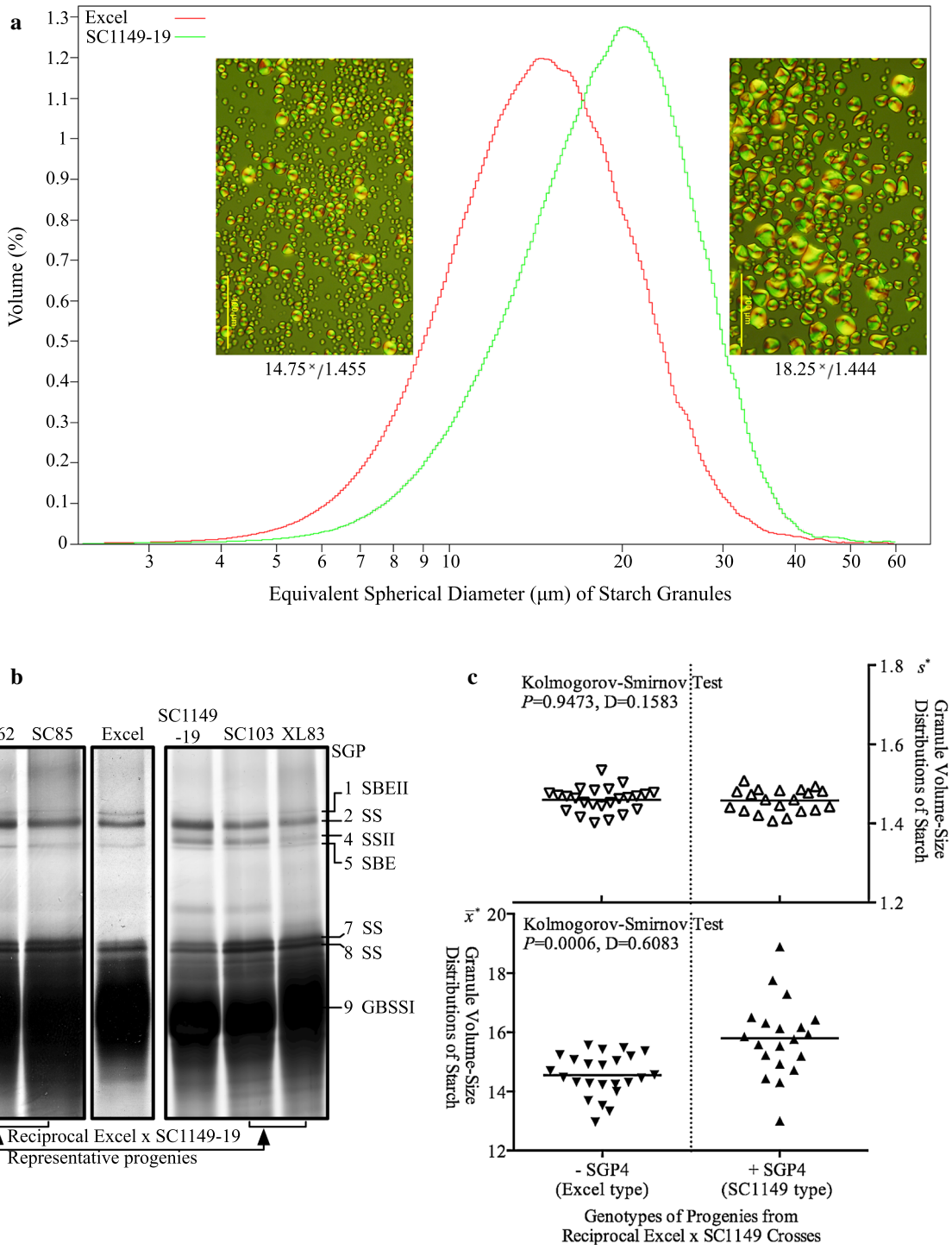

SGP4 locus via SDS-PAGE screening for the null phenotype of SGP4. Please note that the null SGP4 phenotype in the progenies was repeatedly confirmed by SDS-PAGE analyses of multiple starch samples, and by overloading of two and three times of protein extracts from starches of these progenies for all these analyses. Typical SGP profiles of these progenies having or lacking SGP4 were compared to those of parental lines in Fig. 3b. The SGP4 band was found to be absent and present from SGP profiles of 24 and 19 progeny, respectively, which fit a segregation ratio of 1:1 ($P = 0.45$, for $X^2 = 0.5813$). This 1:1 segregation ratio among progenies of the cross indicates that the *SGP4* locus should be heterozygous for a functional and null allele in SC1149-19, but homozygous for the recessive null allele in

◀**Fig. 3** The *SGP4* locus for a homoeologous isoform of starch synthase II is a QTL for the scale ($\bar{x}^*$) of the granule lognormal volume-size distribution of starch in sweetpotatoes. **a** Comparison of granule morphology and lognormal volume-size distributions of starches from two parents, Excel and SC1149-19, of a reciprocal-cross population. Polarized microscopy images of representative starch granule populations from the two lines were displayed at the side of their respective volume-size distribution. The starch samples were prepared from sweetpotatoes of the US No. 1 petite size for both lines that were grown side-by-side in the same season. The sizing of starch granules and smoothing of these distribution curves were carried out as described before. **b** Representative profiles of SGPs from storage roots of the two parents and some of their reciprocal-cross progeny. SGPs were extracted from starch via boiling in a SDS Tris-HCl buffer, fractionated using a modified SDS-PAGE procedure, and visualized with silver staining. The identities of seven SGPs were revealed by peptide sequencing. **c** Graphic summary of statistical comparisons of two datasets each for the $\bar{x}^*$ and s^* factors that specify granule lognormal volume-size distributions of starches from the two genotypic groups of progeny (24 vs. 20) of the reciprocal-cross population. A total of 44 progeny from the population were genotyped at the *SGP4* locus for the presence or absence of SGP4 in starch granules and phenotyped for the $\bar{x}^*$ and s^* of lognormal volume-size distributions of starch granules from their storage roots. The two datasets for $\bar{x}^*$ and s^* were statistically tested for any significant genotype-associated differences using the unpaired nonparametric Kolmogorov–Smirnov test

Excel. Furthermore, relative to the *SGP4* locus, the reciprocal crosses between the two parental lines were in effect a test cross.

We further examined whether two phenotypic groups of $\bar{x}^*$ or s^* of the granule lognormal volume-size distributions of starches from the two genotypic groups having or lacking SGP4 differed significantly from each other. Figure 3c summarizes the statistical test results using unpaired nonparametric K–S tests against the null hypothesis of samples drawn from the same distribution. The two groups of s^* values did not differ significantly from each other ($P = 0.9473$, $D = 0.153$). Moreover, the s^* values did not differ significantly within each group (CV = 0.0208 and 0.02338 for the group means of 1.452 and 1.460, respectively) or from those of starches from the two parents. This indicated that the shape of the granule lognormal volume-size distributions of starch was inherited intact in the population and not affected by the loss of the SSII homoeolog. However, the two groups of $\bar{x}^*$ values differed significantly ($P = 0.0006$, $D = 0.6083$). The null phenotype of *SGP4* was tightly associated with the group of $\bar{x}^*$ having a smaller group mean of 14.85 μm, and was thus most likely responsible for the downsizing of the $\bar{x}^*$ (14.75 μm) of the granule lognormal volume-size distribution of starch in Excel as compared with that (18.25 μm) in SC1149-19. Therefore, the *SGP4* locus is most likely a QTL modulating the scale of the granule lognormal volume-size distribution of starch in sweetpotatoes.

Discussion

In this study, we demonstrated that starch granule sizes in storage tissues, when determined in high resolution and specified properly as a frequency distribution function, could provide useful information on the process of granule formation and growth. In particular, the finding of the self-preserving lognormal volume-size distributions of starch granules in developing sweetpotatoes provided evidence for the involvement of agglomeration during formation and growth of starch granules. Furthermore, the identification of the *SSII* locus as a QTL modulating the scale of the granule volume-size distribution demonstrated for the first time a direct impact of a starch synthesis enzyme on starch granule size distributions.

A new approach for properly defining starch granule sizes

The heterogeneous shapes, very low sphericity and distributed sizes of starch granules in sweetpotatoes, just as in starch-accumulating tissues of many other plant species, presented major challenges in accurate determination and proper specification of granule sizes. Careful comparison of the three commonly used methods for sizing starch granules showed that the Coulter (or the electrical sensing zone, ESZ) method is the only one that yielded satisfactory repeatability for sizing the same sweetpotato starch samples (CV <2.5 %). It is likely due to the fact that the Coulter method is not affected by particle shape, color, composition and reflective index as it is based on measuring the particle-volume-dependent increase in electric resistance by particles passing through an aperture between two electrodes. Moreover, sizing of granules in an electrolyte suspension under constant stirring helped preventing re-agglomeration and pelleting of granules to ensure a well-dispersed granule suspension for representative random sampling. The high-resolution and high-accuracy sizing of a large number of starch granules ($>2.5 \times 10^5$ per measurement) using the Coulter method also yield representative granule volume-size distributions of sweetpotato starch in sufficiently high resolution to allow detection of differences in both scale and shape of the granule size distributions.

Since the measured granule volume at each defined size bin in equivalent spherical diameter can be weighted by either the granule number frequency or the total volume (or mass if granule density is known) percentage, there could be either number- or volume-weighted granule size distributions. We argue that the number-weighted granule size distribution is not suited for physiological or genetic studies for the following reasons. First, a number frequency

Table 3 Summary of identification of major starch granule-bound proteins (SGPs) in sweetpotato storage roots by MALDI-TOF/TOF peptide map fingerprint

SGP	SDS-PAGE size (kDa)	Best-hit protein	GeneBank accession	Mr-Matched[a] peptide no.	Hits	Protein score	Sequence coverage (%)	Putative identity	Putative orthologs
1	111	Starch branching enzyme II (*I. batatas*)	BAB40334	13	8	73	21	SBEII	SBEIIb in wheat[b], barley[c], and maize[d]
2	107	Starch synthase (*I. batatas*)	AAC19119	17	1	176	37	SSII	SSIIa in wheat[b], barley[c], and maize[d]
4	99	Starch synthase (*I. batatas*)	AAC19119	12	1	107	28	SSII	SSIIa in wheat[b], barley[c], and maize[d]
5	97	Starch branching enzyme II (*I. batatas*)	BAB40334	14	1	107	21	SBEII	SBEIIb in wheat[b], barley[c], and maize[d]
7	70	Starch synthase (*S. tuberosum*)	CAA58220	7	19	57	12	SSI (?)	SSI in wheat[b], barley[c], and maize[d]
8	68	Granule-bound starch synthase I (*I. batatas*)	BAB68126	11	1	146	24	GBSSI	GBSSI in wheat[b], barley[c], maize[d], and other species[e]
9	60	Granule-bound starch synthase I (*I. batatas*)	AAA86423	17	1	457	40	GBSSI	GBSSI in wheat[b], barley[c], maize[d], and other species[e]
10	55	Granule-bound starch synthase I (*I. batatas*)	Q42857	7	3	167	14	GBSSI	GBSSI in wheat[b], barley[c], maize[d], and other species[e]
12	65	Granule-bound starch synthase I (*I. batatas*)	Q42857	9	1	127	19	GBSSI	GBSSI in wheat[b], barley[c], maize[d], and other species[e]

[a] Match between the observed monoisotopic mass (Mr) of a peptide from a query protein and the Mr-expt or the Mr-calc, i.e., the experimental or calculated monoisotopic mass of a noncharged peptide in the hit protein

[b] Peng et al. (2000), Rahman et al. (1995), Regina et al. (2005)

[c] Borén et al. (2004)

[d] Grimaud et al. (2008), Mu-Forster et al. (1996)

[e] Baldwin (2001)

for an arbitrarily defined size bin may not have any direct physiological or genetic relevance. Second, the number of small granules generated from fragmented granules during isolation, which could not be detected or separated, will distort both the scale and shape of the granule number size distributions to a much greater degree than those of a volume or mass size distribution. For all sweetpotato starch samples sized in this study, granules having an equivalent spherical diameter of less than 5.5 μm represented approximately 30 % of the total number of granules but only about 1 % of the total volume of all granules (of any size), as calculated from instrument output data. Thus, when expressed as a differential volume percentage, the granule volume-size distribution should have much less chance to be significantly skewed by a comparatively very small volume percentage of those fragmented granules in small-size bins. At last, the differential volume (or mass) percentage of starch granules at a certain size is apparently physiologically and genetically relevant in relation to starch biosynthesis.

We further adopted the use of the geometric mean $\bar{x}^*$ and the multiplicative standard deviation s^* in the $\bar{x}^* \times /s^*$ form (Limpert et al. 2001) to specify granule lognormal volume-size distributions of sweetpotato starch instead of using one scale parameter or two traditional parameters μ (the graphic mean) and σ (the graphic standard deviation) in the logarithms. This specification has the following advantages. First, the scale estimator $\bar{x}^*$ and the shape factor s^* correspond to the geometric mean and geometric standard deviation calculated by the instrument software and thus do not require any further mathematical transformation. Second, this multiplicative specification intuitively depicts the interaction between the central tendency and the spread of the volume-weighted sizes of starch granules in a population. Corresponding to $\bar{x} \pm s$, $\bar{x} \pm 2s$, and $\bar{x} \pm 3s$ intervals of a normal distribution, intervals of a lognormal distribution specified in the multiplicative forms of $\bar{x}^* \times /s^*$, $\bar{x}^* \times /(s^*)^2$, and $\bar{x}^* \times /(s^*)^3$ cover approximately 68.3, 95.5, and 99.7 % confidence intervals of a lognormal distribution, respectively. Third, since $\bar{x}^*$ is in the form of volume-equivalent spherical diameter and s^* is dimensionless, these parameters can be thus used to universally compare various granule volume-size distributions in starch-accumulating tissues of the same or different species. More importantly, we demonstrated that the two parameters are quantitative traits and useful physiological indexes.

Characteristics of granule lognormal volume-size distributions of starches in developing sweetpotatoes

Several lines of evidence demonstrate that the scale ($\bar{x}^*$) and the shape (s^*) of granule lognormal volume-size distributions of starch in sweetpotatoes are independently variable. This implies that there may be two categories of physiological and/or genetic factors that either impact the growth capacity of starch granules or scatter the volume sizes of starch granules. First, granule lognormal volume-size distributions of starches from some analyzed sweetpotato genotypes shared similar $\bar{x}^*$, but differed significantly in s^*, whereas those from some other genotypes displayed the opposite tendency. Second, the loss of one of three homoeologous SSIIs in sweetpotatoes was found to be genetically associated with downsizing only the scale ($\bar{x}^*$) of the granule volume-size distribution. At last, the shape (s^*) but not the scale ($\bar{x}^*$) of granule lognormal volume-size distributions of starch was significantly and inversely correlated with the apparent amylose contents of starch (Table 1). Higher amylose contents in starch granules appeared to be associated with a narrower volume-size distribution of starch granules.

The impact of the amylose content on granule sizes has been noticed in previous studies. The 'average sizes' of starch granules in high-amylose barley (Walker 1969), wrinkled peas (Greenwood and Thomson 1962), and maize *ae* mutant endosperm (Boyer et al. 1976; Garwood and Creech 1972; Katz et al. 1993; Wang et al. 1993) have been reported to be smaller than normal at all developmental stages. However, the simple number-averaged sizes (with as few as 30 sampled granules) for starch granule populations in these studies could not be representative of the granule size distributions of those high-amylose starch. New studies on granule size distributions of these starches with sufficient resolution are needed to properly determine the effect of higher amylose contents on granule sizes of these starches. Moreover, both the scale ($\bar{x}^*$) and the shape (s^*) of granule lognormal volume-size distributions were not found in this study to correlate with any thermal properties of sweetpotato starches, which were not in line with the conclusion that granule sizes affected the thermal properties of starch in several previous studies (Ao and Jane 2007; Karlsson et al. 1983; Lindeboom et al. 2004; Singh and Kaur 2004). This discrepancy may have resulted from differences in determination and specification of the granule size distributions.

Perhaps the most important finding of this study was that the granule lognormal volume-size distributions of starch in developing sweetpotato storage roots attained a self-preserving state, i.e., staying invariant in the s^* but upsizing the $\bar{x}^*$, as summarized in Fig. 2. The self-preserving lognormal size distributions are well known to be specifically associated with particles undergoing agglomeration (Friedlander and Wang 1966; Lehtinen and Zachariah 2001; Tambo and Watanabe 1979; Vemury and Pratsinis 1995; Wang and Friedlander 1967), which refers to the process of formation of more or less firmly bound particles by collisions between primary particles, primary particles

and agglomerates, and pre-existing agglomerates (Flagan and Mori 2007; Stroh 1993). Therefore, the self-preserving kinetics of granule lognormal volume-size distributions of starch in developing sweetpotato storage roots provided a strong piece of evidence for the involvement of agglomeration in the formation and growth of starch granules. Indeed, small particles, the coacervate droplets, were observed to accumulate and then decline with the formation of starch granules in the amyloplast (Badenhuizen 1965, 1973). Please note that the widely accepted mechanism of growth of starch granules by apposition, which is the process of gradual centrifugal (or layer-wise) deposition of glucan polymers on the surface of a growing granule, can be regarded as one type of agglomeration, i.e., agglomeration between a primary particle and agglomerates. Whether other types of agglomeration such as coagulation, flocculation, and those between sub-granule particles are also involved in the formation and growth of starch granules awaits further studies. Future studies of kinetics of granule lognormal volume-size distributions of starch in developing starch-accumulating tissues, especially those of mutants deficient in starch synthesis, could provide insights into the formation and growth of starch granules.

The scale ($\bar{x}^*$) and shape (s^*) of lognormal volume-size distributions of starch granules relate granule sizes to starch biosynthesis

The multiplicative two-parameter specification for granule size distributions also proved to be a useful tool for proper quantitative evaluation of genotypic effects of starch biosynthesis enzymes on both the shape and the scale of granule size distributions in a plant tissue. As summarized in Fig. 3, one of the homoeologous SSII loci was shown to be a QTL for only the scale ($\bar{x}^*$) of granule lognormal volume-size distributions of starch in sweetpotatoes. This result also indicated that the genetic redundancy of starch synthesis enzymes conferred by homoeologous loci in the hexaploid sweetpotato increased the growth rate of all starch granules, but did not alter the spread of volume sizes of starch granules. In fact, sufficiently longer growth for storage roots of Excel could eventually offset the effects of downsizing of the $\bar{x}^*$ of granule lognormal volume-size distributions of starch conferred by the loss of one dose of SSII (data not shown), which was similar in effect to the expansion of the scale of self-preserving lognormal granule volume-size distributions of starch in bulking storage roots of SC1149-19 (Fig. 2).

On the other hand, deficiencies in other starch synthesis enzymes or regulatory elements in mutant tissues may affect only the shape s^* or both the shape and scale of granule volume-size distributions of starch. It has been reported that the loss of a soluble starch synthase SSIV resulted in a drastic reduction in granule number per plastid, but an increase in granule sizes in leaf tissues of an Arabidopsis mutant (Crumpton-Taylor et al. 2013; Roldan et al. 2007). Although the result cannot be directly extrapolated as theses studies were either not at the level of granule population in a tissue, or used different specification for granule size distribution, it does suggest that both the scale and shape of granule volume-size distributions in the mutant leave tissue could be affected since the decrease in granule number per plastid would theoretically affect the spread of granule size distribution by altering the number frequency and volume percentages of granules at various sizes. Since starch granules exist in distributed sizes in plant tissues, the shape of the granule size distributions, which defining the spread of distributed sizes, have to be equally analyzed along with the sizes in any studies concerning starch granule sizes for any meaningful conclusions. The multiplicative two-parameter specification integrally define the scale and the shape of granule size distributions in one simple form, and thus could prove to be a useful tool in future studies concerning starch granule sizes.

Characteristics of SGPs in sweetpotato storage roots

The major types of SGPs in sweetpotato storage roots, including two or three starch synthase isoforms and one SBE isoform, resemble those in maize (Mu-Forster et al. 1996) and rice (Umemoto and Aoki 2005) endosperm, rather than those in similar underground potato tubes (Edwards et al. 1995; Ritte et al. 2002). It is unclear whether this similarity has any biological implications. The presence of a disproportionately large amount of GBSSI, as well as multiple homoeologous and paralogous isoforms of GBSSI in sweetpotato starch granules is quite unique. Although GBSSI is also the most predominant granule-bound protein in all normal starch varieties of various plant species that have been analyzed to date (Baldwin 2001), GBSSI is generally encoded by a single-copy gene, the so-called *Waxy* gene, in most species. This apparently larger amount of GBSSI in sweetpotato starch granules, however, was not accompanied by a higher amount of amylose, which is synthesized exclusively by GBSSI (Ball et al. 1998). The amylose content among starch samples from 22 sweetpotato cultivars/clones ranged from 18.11 to 29.56 % (Table 1), consistent with those from normal potatoes (20.1–31.0 %), corn (22.4–32.5 %), and wheat (18–30 %) (Singh et al. 2003). Thus, the increased amount of GBSSI due to the genetic redundancy of gene duplications and hexaploidy in sweetpotatoes may have augmented the synthesis rate, but not the amount of amylose in amyloplasts.

Author contribution statement MG conceived and designed all the experiments, performed at least initial phases of all experiments including most of the ESZ granule sizing and the analyses and interpretation of all data, and wrote the manuscript. QX performed microscopy imaging of starch granule, image sizing analyses, and review of the manuscript. AWA performed part of starch extraction and major part of SDS-PAGE analyses of SGPs including genotyping. LS performed part of the ESZ granule sizing. GMA performed part of starch extraction, and prepared pot-grown sweetpotatoes. VN prepared part of field-grown sweetpotatoes.

Acknowledgments This work was supported by the National Institute of Food and Agriculture, US Department of Agriculture (Grant Numbers 2009-38863-2054 to MG, QX, and VN, 2014-38821-22429 to MG). We would like to thank Dr. Yoonsung Jung for assistance and helpful discussions on all statistical issues in the study, and Celestine Fosung, Adeline Douanla, and Lakshmi Yellapragada for technical assistance.

Compliance with ethical standards

Conflict of interest The authors declare no conflicts of interest.

References

Ao Z, Jane J-l (2007) Characterization and modeling of the A- and B-granule starches of wheat, triticale, and barley. Carbohydr Polym 67:46–55. doi:10.1016/j.carbpol.2006.04.013

Badenhuizen NP (1965) Occurrence and development of starch in plants. In: Whistler RL, Paschall EF (eds) Starch: chemistray and technology, vol I, 1st edn. Academic Press, New York, pp 65–103

Badenhuizen NP (1973) Fundamental problems in the biosynthesis of starch granules. Ann N Y Acad Sci 210:11–16

Baldwin PM (2001) Starch granule-associated proteins and polypeptides: a review. Starch Stärke 53:475–503. doi:10.1002/1521-379x(200110)53:10<475

Ball SG, Morell MK (2003) From bacterial glycogen to starch: understanding the biogenesis of the plant starch granule. Annu Rev Plant Biol 54:207–233

Ball SG, van de Wal MHBJ, Visser RGF (1998) Progress in understanding the biosynthesis of amylose. Trends Plant Sci 3:462–467

BeMiller JN, Whistler RL (2009) Starch: chemistry and technology. Academic Press, New York

Borén M, Larsson H, Falk A, Jansson C (2004) The barley starch granule proteome—internalized granule polypeptides of the mature endosperm. Plant Sci 166:617–626

Boyer CD, Shannon JC, Garwood DL, Creech RG (1976) Changes in starch granule size and amylose percentage during kernel development in several *Zea mays* L. genotypes. Cereal Chem 53:327–337

Buléon A, Colonna P, Planchot V, Ball S (1998) Starch granules: structure and biosynthesis. Int J Biol Macromol 23:85–112. doi:10.1016/S0141-8130(98)00040-3

Chen Z, Schols HA, Voragen AGJ (2003) Starch granule size strongly determines starch noodle processing and noodle quality. J Food Sci 68:1584–1589. doi:10.1111/j.1365-2621.2003.tb12295.x

Copeland L, Blazek J, Salman H, Tang MC (2009) Form and functionality of starch. Food Hydrocolloids 23:1527–1534. doi:10.1016/j.foodhyd.2008.09.016

Crumpton-Taylor M et al (2013) Starch synthase 4 is essential for coordination of starch granule formation with chloroplast division during Arabidopsis leaf expansion. New Phytol. doi:10.1111/nph.12455

Dai ZM (2009) Starch granule size distribution in grains at different positions on the spike of wheat (*Triticum aestivum* L.). Starch Stärke 61:582–589. doi:10.1002/Star.200800112

Edwards A, Marshall J, Sidebottom C, Visser RGF, Smith AM, Martin C (1995) Biochemical and molecular characterization of a novel starch synthase form potato tubers. Plant J 8:283–294

Edwards MA, Osborne BG, Henry RJ (2008) Effect of endosperm starch granule size distribution on milling yield in hard wheat. J Cereal Sci 48:180–192. doi:10.1016/J.Jcs.2007.09.001

Emes MJ, Bowsher CG, Hedley C, Burrell MM, Scrase-Field ES, Tetlow IJ (2003) Starch synthesis and carbon partitioning in developing endosperm. J Exp Bot 54:569–575

Flagan CR, Mori Y (2007) Creation of praticles by reaction. In: Masuda H, Higashitani K, Yoshida H (eds) Powder technology—fundamentals of particles, powder beds, and particle generation. CRC Press, New York, p 413

Friedlander SK, Wang CS (1966) The self-preserving particle size distribution for coagulation by Brownian motion. J Colloid Interface Sci 22:126–132. doi:10.1016/0021-9797(66)90073-7

Gao M, Ashu G, Stewart L, Akwe W, Njiti V, Barnes S (2010) *Wx* intron variations support an allohexaploid origin of the sweetpotato [*Ipomoea batatas* (L.) Lam]. Euphytica. doi:10.1007/s10681-010-0275-z

Garwood DL, Creech RG (1972) Kernel phenotypes of *Zea mays* L. genotypes possessing one to four mutated genes. Crop Sci 12:119–121

Goering KJ, Fritts DH, Eslick RF (1973) A study of starch granule size and distribution in 29 barley varieties. Starch Stärke 25:297–302

Greenwood C, Thomson J (1962) Studies on the biosynthesis of starch granules. 2. The properties of the components of starches from smooth-and wrinkled-seeded peas during growth. Biochem J 82:156

Grimaud F, Rogniaux H, James MG, Myers AM, Planchot V (2008) Proteome and phosphoproteome analysis of starch granule-associated proteins from normal maize and mutants affected in starch biosynthesis. J Exp Bot 59:3395–3406. doi:10.1093/jxb/ern198

Hannah LC, James M (2008) The complexities of starch biosynthesis in cereal endosperms. Curr Opin Biotechnol 19:160–165. doi:10.1016/j.copbio.2008.02.013

Hoover R (2001) Composition, molecular structure, and physicochemical properties of tuber and root starches: a review. Carbohydr Polym 45:253–267. doi:10.1016/S0144-8617(00)00260-5

James MG, Denyer K, Myers AM (2003) Starch synthesis in the cereal endosperm. Curr Opin Plant Biol 6:215–222

Jeon JS, Ryoo N, Hahn TR, Walia H, Nakamura Y (2010) Starch biosynthesis in cereal endosperm. Plant Physiol Biochem 48:383–392. doi:10.1016/j.plaphy.2010.03.006

Karlsson R, Olered R, Eliasson AC (1983) Changes in starch granule size distribution and starch gelatinization properties during development and maturation of wheat, barley and rye. Starch Stärke 35:335–340. doi:10.1002/star.19830351002

Katz F, Furcsik S, Tenbarge F, Hauber R, Friedman R (1993) Behavior of starches derived from varieties of maize containing different genetic mutations: effects of starch genotype on granular morphology. Carbohydr Polym 21:133–136

Keeling PL, Myers AM (2010) Biochemistry and genetics of starch synthesis. Ann Rev Food Sci Technol 1:271–303

Lehtinen KE, Zachariah MR (2001) Self-preserving theory for the volume distribution of particles undergoing Brownian coagulation. J Colloid Interface Sci 242:314–318

Li W-Y et al (2008) Comparison of starch granule size distribution between hard and soft wheat cultivars in Eastern China. Agric Sci China 7:907–914. doi:10.1016/s1671-2927(08)60129-7

Li X-Q, Zhang J, Luo S, Liu G, Murphy A, Leclerc Y, Xing T (2011) Effects of sampling methods on starch granule size measurement of potato tubers under a light microscope. Int J Plant Biol 2:5

Limpert E, Stahel WA, Abbt M (2001) Log-normal distributions across the sciences: keys and clues. Bioscience 51:341–352. doi:10.1641/0006-3568(2001)051[0341:Lndats]2.0.Co;2

Lindeboom N, Chang PR, Tyler RT (2004) Analytical, biochemical and physicochemical aspects of starch granule size, with emphasis on small granule starches: a review. Starch Stärke 56:89–99. doi:10.1002/star.200300218

Moorthy SN (2002) Physicochemical and functional properties of tropical tuber starches: a review. Starch Stärke 54:559–592. doi:10.1002/1521-379X(200212)54:12<559

Mu-Forster C et al (1996) Physical association of starch biosynthetic enzymes with starch granules of maize endosperm (granule-associated forms of starch synthase I and starch branching enzyme II). Plant Physiol 111:821–829

Park SH, Wilson JD, Seabourn BW (2009) Starch granule size distribution of hard red winter and hard red spring wheat: its effects on mixing and breadmaking quality. J Cereal Sci 49:98–105. doi:10.1016/J.Jcs.2008.07.011

Peng M, Gao M, Båga M, Hucl P, Chibbar RN (2000) Starch-branching enzymes preferentially associated with A-type starch granules in wheat endosperm. Plant Physiol 124:265–272

Perez S, Bertoft E (2010) The molecular structures of starch components and their contribution to the architecture of starch granules: a comprehensive review. Starch Stärke 62:389–420. doi:10.1002/Star.201000013

Rahman S et al (1995) The major proteins of wheat endosperm starch granules. Aust J Plant Physiol 22:793–803

Regina A et al (2005) Starch branching enzyme IIb in wheat is expressed at low levels in the endosperm compared to other cereals and encoded at a non-syntenic locus. Planta 222:899–909. doi:10.1007/s00425-005-0032-z

Ritte G, Lloyd JR, Eckermann N, Rottmann A, Kossmann J, Steup M (2002) The starch-related R1 protein is an α-glucan, water dikinase. Proc Natl Acad Sci USA 99:7166–7171

Roldan I et al (2007) The phenotype of soluble starch synthase IV defective mutants of *Arabidopsis thaliana* suggests a novel function of elongation enzymes in the control of starch granule formation. Plant J 49:492–504. doi:10.1111/j.1365-313X.2006.02968.x

Shannon JC, Garwood DL (1984) Genetics and physiology of starch development. In: Wishtler RL, Bemiller JN, Paschall EF (eds) Starch: chemistry and technology. Academic Press, Orlando, pp 25–86

Singh N, Kaur L (2004) Morphological, thermal, rheological and retrogradation properties of potato starch fractions varying in granule size. J Sci Food Agric 84:1241–1252. doi:10.1002/jsfa.1746

Singh N, Singh J, Kaur L, Singh Sodhi N, Singh Gill B (2003) Morphological, thermal and rheological properties of starches from different botanical sources. Food Chem 81:219–231. doi:10.1016/S0308-8146(02)00416-8

Smith AM (2001) The biosynthesis of starch granules. Biomacromolecules 2:335–341

Smith AM, Zeeman SC, Smith SM (2005) Starch degradation. Ann Rev Plant Biol 56:73–98. doi:10.1146/Annurev.Arplant.56.032604.144257

Stroh G (1993) The Effect of coagulation and flocculation on the filtration properites of suspensions incorporating a high content of fines. In: Dobias B (ed) Coagulation and flocculation: theory and applications, vol 47. Marcel Dekker Inc, New York, p 653

Tambo N, Watanabe Y (1979) Physical aspect of flocculation process—I: fundamental treatise. Water Res 13:429–439

Tester RF, Debon SJ (2000) Annealing of starch—a review. Int J Biol Macromol 27:1–12

Tester RF, Karkalas J, Qi X (2004) Starch—composition, fine structure and architecture. J Cereal Sci 39:151–165. doi:10.1016/j.jcs.2003.12.001

Tetlow IJ (2011) Starch biosynthesis in developing seeds. Seed Sci Res 21:5–32. doi:10.1017/s0960258510000292

Tomlinson K, Denyer K (2003) Starch synthesis in cereal grains. Adv Bot Res 40:1–61. doi:10.1016/S0065-2296(05)40001-4

Umemoto T, Aoki N (2005) Single-nucleotide polymorphisms in rice starch synthase IIa that alter starch gelatinisation and starch association of the enzyme. Funct Plant Biol 32:763–768

Vemury S, Pratsinis SE (1995) Self-preserving size distributions of agglomerates. J Aerosol Sci 26:175–185

Walker J (1969) Genetic control of abnormal starch granules and high amylose content in a mutant of Glacier barley. Nature 221:482–483

Wang C, Friedlander S (1967) The self-preserving particle size distribution for coagulation by Brownian motion: II. Small particle slip correction and simultaneous shear flow. J Colloid Interface Sci 24:170–179

Wang YJ, White P, Pollak L, Jane JL (1993) Characterization of starch structures of 17 maize endosperm mutant genotypes with Oh43 inbred line background. Cereal Chem 70:171–179

Wilson JD, Bechtel DB, Todd TC, Seib PA (2006) Measurement of wheat starch granule size distribution using image analysis and laser diffraction technology. Cereal Chem 83:259–268. doi:10.1094/Cc-83-0259

Zeeman SC, Kossmann J, Smith AM (2010) Starch: its metabolism, evolution, and biotechnological modification in plants. Ann Rev Plant Biol 61:209–234. doi:10.1146/Annurev-Arplant-042809-112301

Zhao XC, Sharp PJ (1996) An improved 1-D SDS-PAGE method for the identification of three bread wheat 'waxy' proteins. J Cereal Sci 23:191–193

Zobel H (1988) Molecules to granules: a comprehensive starch review. Starch Stärke 40:44–50